Supplement of Atmos. Chem. Phys. Discuss., 15, 20521–20559, 2015
http://www.atmos-chem-phys-discuss.net/15/20521/2015/
doi:10.5194/acpd-15-20521-2015-supplement

Atmospheric Chemistry and Physics
Discussions
Open Access

Supplement of

Size-resolved measurements of ice nucleating particles at six locations in North America and one in Europe

R. H. Mason et al.

Correspondence to: A. K. Bertram (bertram@chem.ubc.ca)

S1 Calculations of fractions of INPs larger than 1, 1.2, or 2.5 µm from previous studies

S1.1 Vali (1966)

The size distribution of INPs found in hail melt water was reported by Vali (1966). Hail from Alberta, Canada was melted and some of this water was passed through filters of either 0.01 or 1.2 µm pore size. Samples were then analyzed using a drop freezing method. The concentration of INPs in the immersion mode as a function of temperature was given in Fig. 3 of that study for three size ranges: unfiltered, 1.2 µm filtered, and 0.01 µm filtered hail melt water. To calculate the fraction of INPs > 1.2 µm at -12.8 °C (the lowest temperature available and therefore the closest to -15 °C), the concentration of INPs in the 1.2 µm-filtered sample was first divided by the concentration of INPs in the unfiltered sample at this temperature. This fraction was then subtracted from unity.

S1.2 Rosinski et al. (1986)

The size distributions of INPs active in the immersion and condensation nucleation modes over the central and western South Pacific Ocean were determined by Rosinski et al. (1986). Aerosol particle samples were size-selected by an Anderson cascade impactor (similar in principle to the MOUDI) where the stage size cuts were 8, 6, 5, 4, 1, and 0.5 µm. There were also two after filters connected to the impactor in parallel to collect particles smaller than 0.5 µm. Samples were analyzed using either the drop freezing method (immersion mode) or a dynamic developing chamber (condensation mode).

Immersion mode freezing data for twelve samples was reported in Tables 1–12 of Rosinski et al. (1986) with each table corresponding to a different sampling period. As filter measurements were not reported for all samples and it is unclear whether differences in the size of deposits between the impactor and filter samples was accounted for during immersion freezing measurements, here we focus on the impactor samples for the immersion freezing data. We also assume that the freezing of a drop was caused by the presence of a single INP. The fraction of INPs > 1 μm was calculated for each sample in 0.1 °C intervals, and these values were then averaged over all samples. The average fraction of INPs > 1 μm is reported at -10.8 °C. Values are not reported at lower temperatures because of sample saturation.

Condensation mode freezing data was reported in Table 13 of Rosinski et al. (1986). Samples V–VII and IX–XI were used here as these report INP concentrations for all impactor stages, one after filter, and for particles > 1 μm. Although not reported in Table 13, the INP concentrations on the second after filter are assumed to equal those found on the first after filter as instructed in the text. INP concentrations missing from Table 13 were calculated by linear interpolation where possible. The fraction of INPs > 1 μm was first determined for each sample in 1 °C intervals, and then averaged over all samples. The average fraction of INPs > 1 μm is reported at -5 to -6 °C as this is the lowest temperature where data is available for all particle sizes in all samples.

S1.3 Rosinski et al. (1988)

Rosinski et al. (1988) measured the INP size distribution over the Gulf of Mexico by first size selecting aerosol particles with an Andersen cascade impactor with after filters and then analyzing these samples with a dynamic developing chamber. Five size cuts were used for size selection: > 4.5, 3.1, 1.0, 0.4, and 0.1 μm. Figures 2 and 5–7 of that study presented INP concentrations for the condensation freezing mode in twenty samples.

The fraction of INPs > 1 μm was determined in 1 °C intervals within each sample, and then averaged over all samples. In this analysis, sample 1 from August 6, 1986 was excluded as data was missing for particle sizes > 3.1 μm. The average fraction of INPs > 1 μm is reported over -15 to -16 °C. Values were not calculated for lower temperatures due to sample saturation.

S1.4 Berezinski et al. (1988)

The size distribution of INPs active in the condensation nucleation mode over Eastern Europe was determined by Berezinski et al. (1988). Aerosol particle samples were first collect by a cascade impactor with size cuts of 100, 30, 10, 1.0, and 0.1 μm and then analyzed using a thermal diffusion chamber and microscope. Data is presented in Table 1 of that study at freezing temperatures of -8, -10, -12, -15, and -20 °C. Data was used directly from Table 1 to determine the average fraction of INPs > 1 μm. To match the conditions used in this study, the average fraction of INPs > 1 μm is reported for temperatures of -15 and -20 °C.

S1.5 Santachiara et al. (2010)

Santachiara et al. (2010) collected size-resolved aerosol samples on filters by passing ambient air through various sampling heads with size cut-points of either 1, 2.5, or 10 μm. The total suspended particulate was also collected. Aerosol particle samples were then analyzed in a dynamic developing chamber to determine the concentration of INPs active in the condensation mode of freezing. Table 3 of that study presented the fractions of INPs < 1 and < 2.5 μm, which were subtracted from unity here. We report the averaged values between -17 and -19 °C.

S1.6 Huffman et al. (2013)

The size distribution of INPs at a forest site in Colorado was measured by Huffman et al. (2013) using an early iteration of the MOUDI-DFT used in this study. Figure 4 of that study presented INP concentrations as a function of size, which we used to calculate the average fraction of INPs > 1 μm. As was done in Huffman et al. (2013), INP values are reported separately for samples collected during rainfall and samples collected during dry weather. We report the average fraction of INPs > 1 µm at -15 to -20 °C for both sampling conditions.

S1.7 Other studies

Two additional studies reporting INP sizes have not been included here; Bigg and Hopwood (1963) because INP size was calculated based on several assumptions that were not confirmed, and Rosinski et al. (1987) because only the onset freezing temperature was given for each experiment.

S2 Calculating the percentile size of INPs using binned data

The median, 25th percentile, and 75th percentile size of INPs at each location were calculated from the binned MOUDI data shown in Figs. S1–S8 below. The INP sized distribution was first used to find the cumulative INP concentration in each bin from the smallest to the largest aerosol particle size. The following equation was then used to calculate the percentile size of INPs:

$$\text{percentile size of INPs} = l + \left(\frac{pt - c}{f}\right) w \qquad (1)$$

where l is the lower size limit of the bin containing the percentile of interest, p is the desired percentile (p = 0.25, 0.50, and 0.75 for the 25th percentile, median, and 75th percentile, respectively), t is the total INP concentration at a given temperature, c is the cumulative concentration of the preceding bin, and f and w are the INP concentration and width, respectively, of the bin containing the percentile of interest.

References

Berezinski, N. A., Stepanov, G. V. and Khorguani, V. G.: Ice-forming activity of atmospheric aerosol particles of different sizes, Lecture Notes in Physics, edited by P. E. Wagner and G. Vali, 309, 709–712, 1988.

Bigg, E. K. and Hopwood, S. C.: Ice Nuclei in the Antarctic, J. Atmos. Sci., 20, 185–188, 1963.

Huffman, J. A., Prenni, A. J., DeMott, P. J., Pöhlker, C., Mason, R. H., Robinson, N. H., Fröhlich-Nowoisky, J., Tobo, Y., Després, V. R., Garcia, E., Gochis, D. J., Harris, E., Müller-Germann, I., Ruzene, C., Schmer, B., Sinha, B., Day, D. A., Andreae, M. O., Jimenez, J. L., Gallagher, M., Kreidenweis, S. M., Bertram, A. K. and Pöschl, U.: High concentrations of biological aerosol particles and ice nuclei during and after rain, Atmos. Chem. Phys., 13, 6151–6164, doi:10.5194/acp-13-6151-2013, 2013.

Rosinski, J., Haagenson, P. L., Nagamoto, C. T. and Parungo, F.: Ice-forming nuclei of maritime origin, J. Aerosol Sci., 17, 23–46, doi:10.1016/0021-8502(86)90004-2, 1986.

Rosinski, J., Haagenson, P. L., Nagamoto, C. T. and Parungo, F.: Nature of ice-forming nuclei in marine air masses, J. Aerosol Sci., 18, 291–309, doi:10.1016/0021-8502(87)90024-3, 1987.

Rosinski, J., Haagenson, P. L., Nagamoto, C. T., Quintana, B., Parungo, F. and Hoyt, S. D.: Ice-forming nuclei in air masses over the Gulf of Mexico, J. Aerosol Sci., 19, 539–551, doi:10.1016/0021-8502(88)90206-6, 1988.

Santachiara, G., Di Matteo, L., Prodi, F. and Belosi, F.: Atmospheric particles acting as Ice Forming Nuclei in different size ranges, Atmos. Res., 96, 266–272, doi:10.1016/j.atmosres.2009.08.004, 2010.

Vali, G.: Sizes of Atmospheric Ice Nuclei, Nature, 212, 384–385, doi:10.1038/212384a0, 1966.

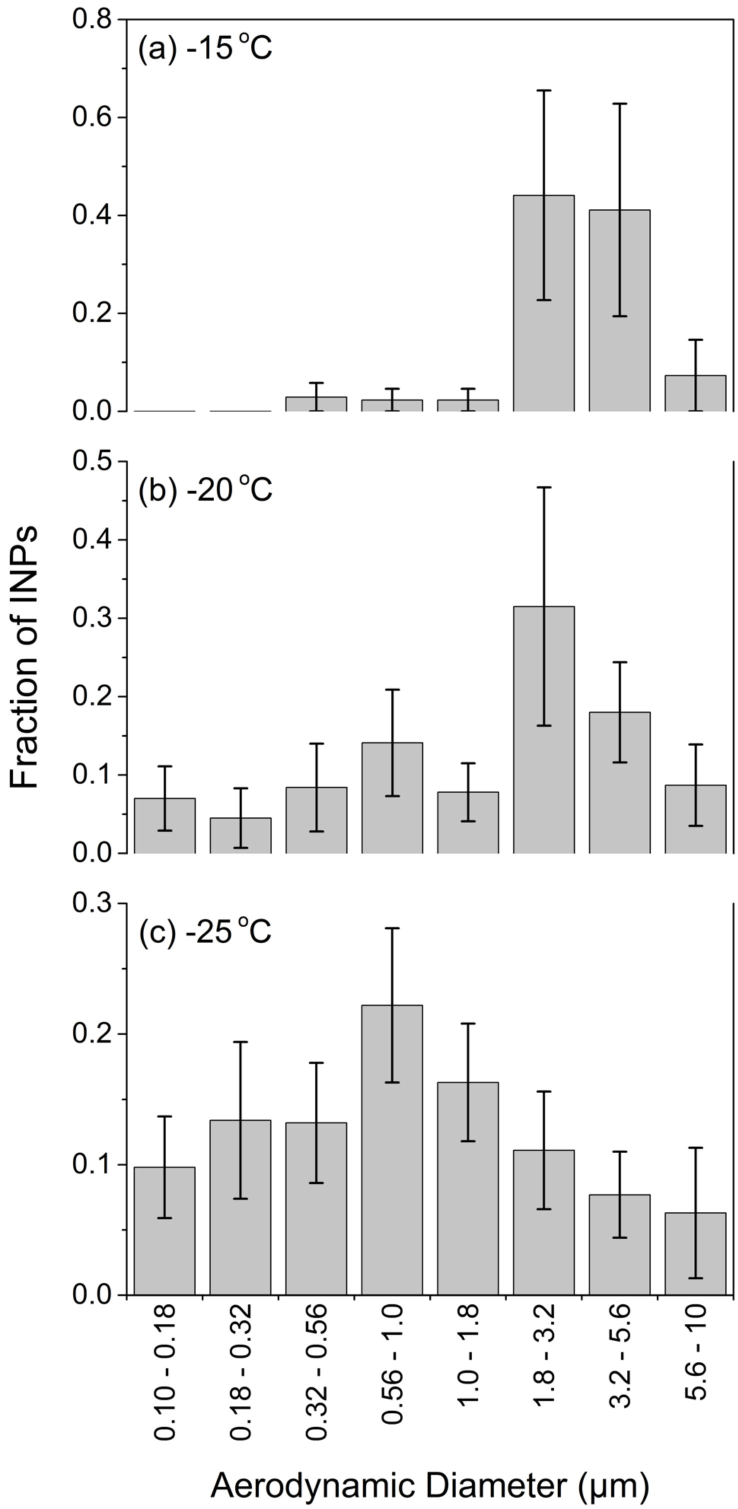

Figure S1. Mean INP size distributions at Alert, NU, Canada at (a) -15°C, (b) -20°C, and (c) -25°C. Here we report the fraction of INPs in each MOUDI size bin as the mean of all samples with uncertainty as the standard error of the mean.

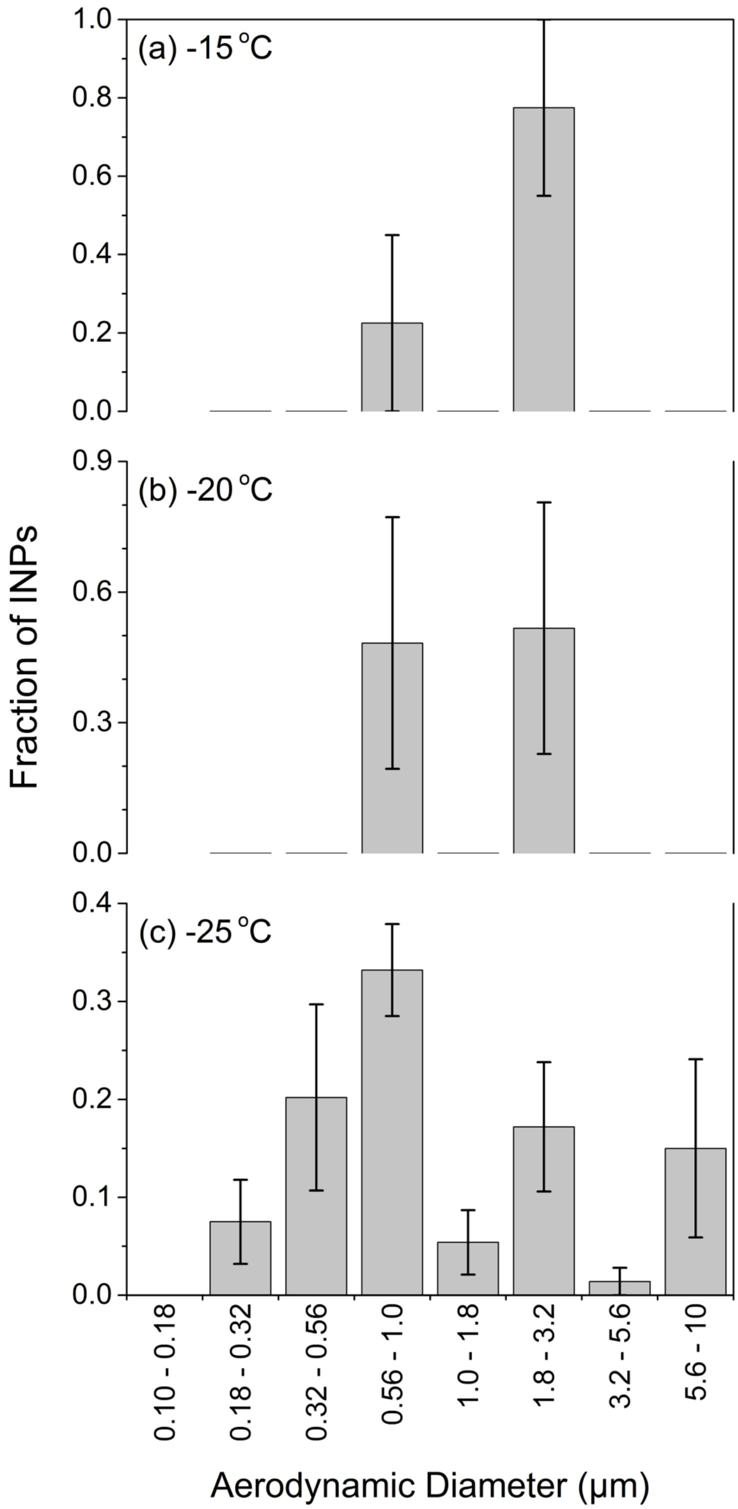

Figure S2. Mean INP size distributions at Whistler Mountain, BC, Canada at (a) -15 °C, (b) -20 °C, and (c) -25 °C. Here we report the fraction of INPs in each MOUDI size bin as the mean of all samples with uncertainty as the standard error of the mean. Number concentrations below 0.18 μm were not measured but plot axes are consistent with the other figures for easier comparison of the size distributions.

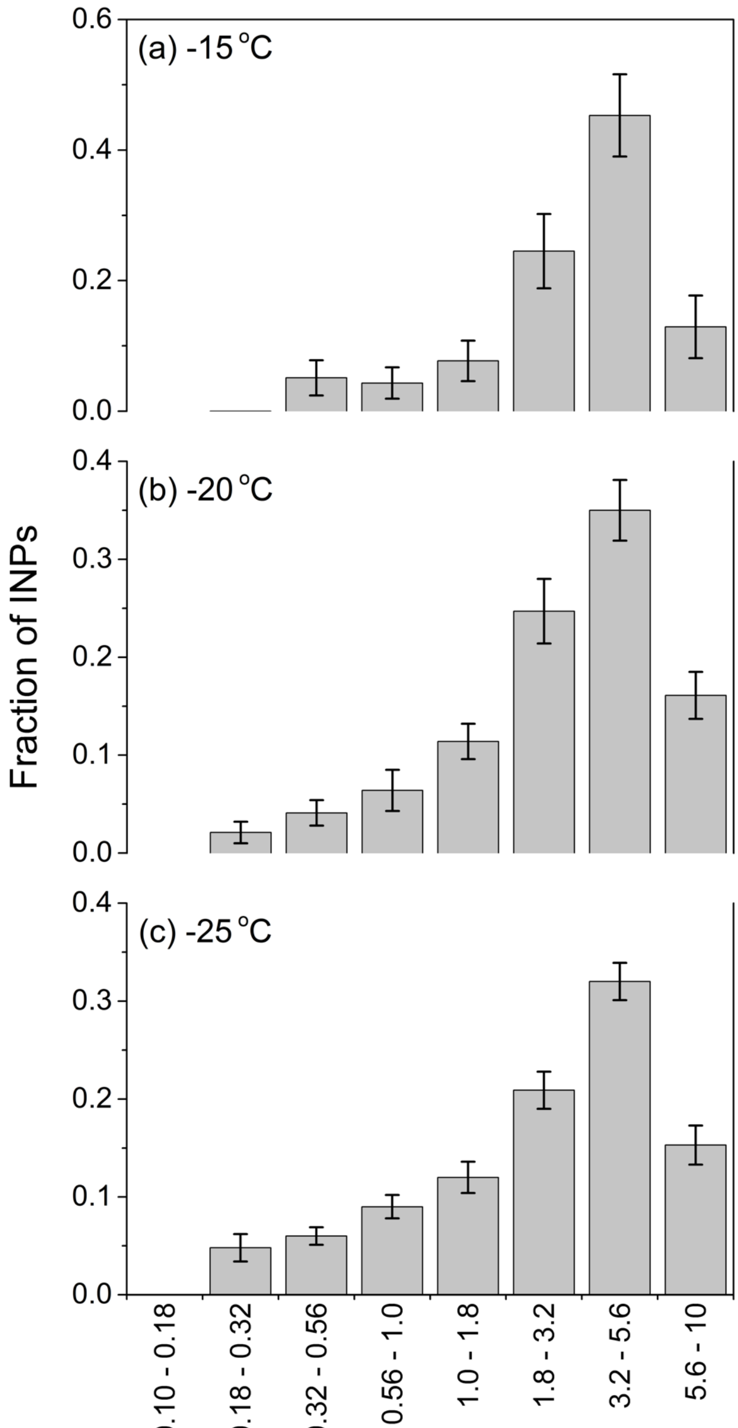

Figure S3. Mean INP size distributions at Amphitrite Point, BC, Canada at (a) -15 °C, (b) -20 °C, and (c) -25 °C. Here we report the fraction of INPs in each MOUDI size bin as the mean of all samples with uncertainty as the standard error of the mean. Number concentrations below 0.18 µm were not measured but plot axes are consistent with the other figures for easier comparison of the size distributions.

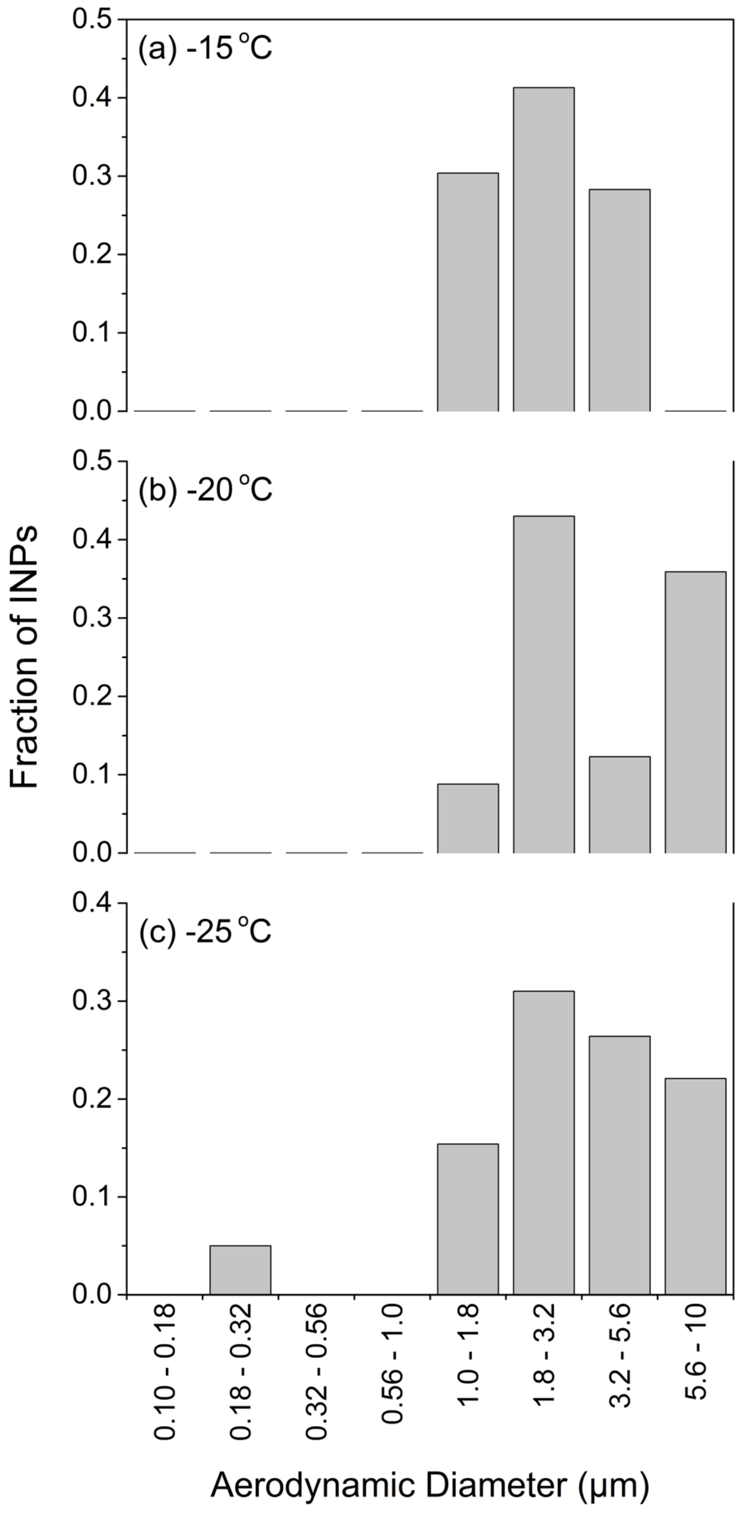

Figure S4. Mean INP size distributions at the Labrador Sea at (a) -15 °C, (b) -20 °C, and (c) -25 °C. Here we report the fraction of INPs in each MOUDI size bin as the mean of all samples with uncertainty as the standard error of the mean. As only one sample was collected at this location, no experimental uncertainty is reported.

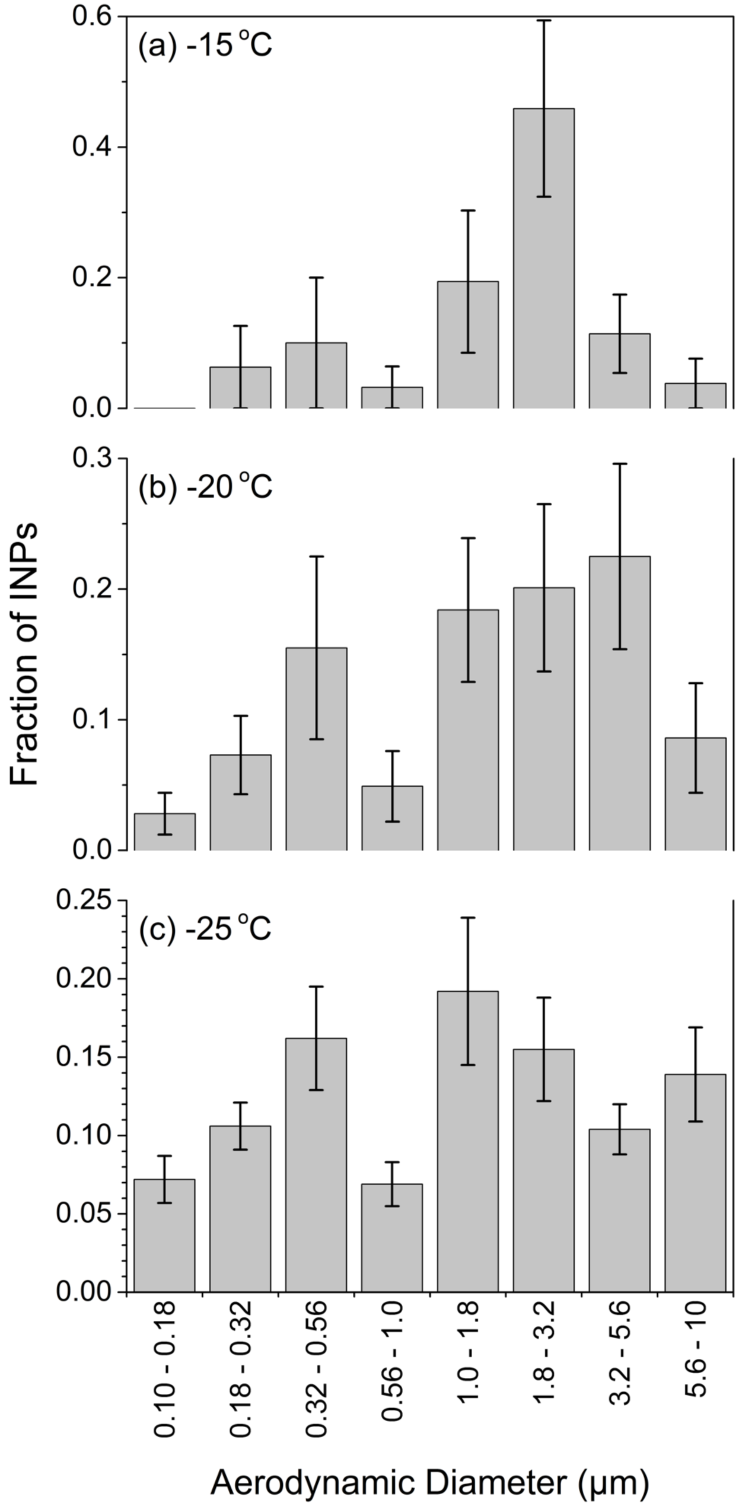

Figure S5. Mean INP size distributions at Saclay, France at (a) -15 °C, (b) -20 °C, and (c) -25 °C. Here we report the fraction of INPs in each MOUDI size bin as the mean of all samples with uncertainty as the standard error of the mean.

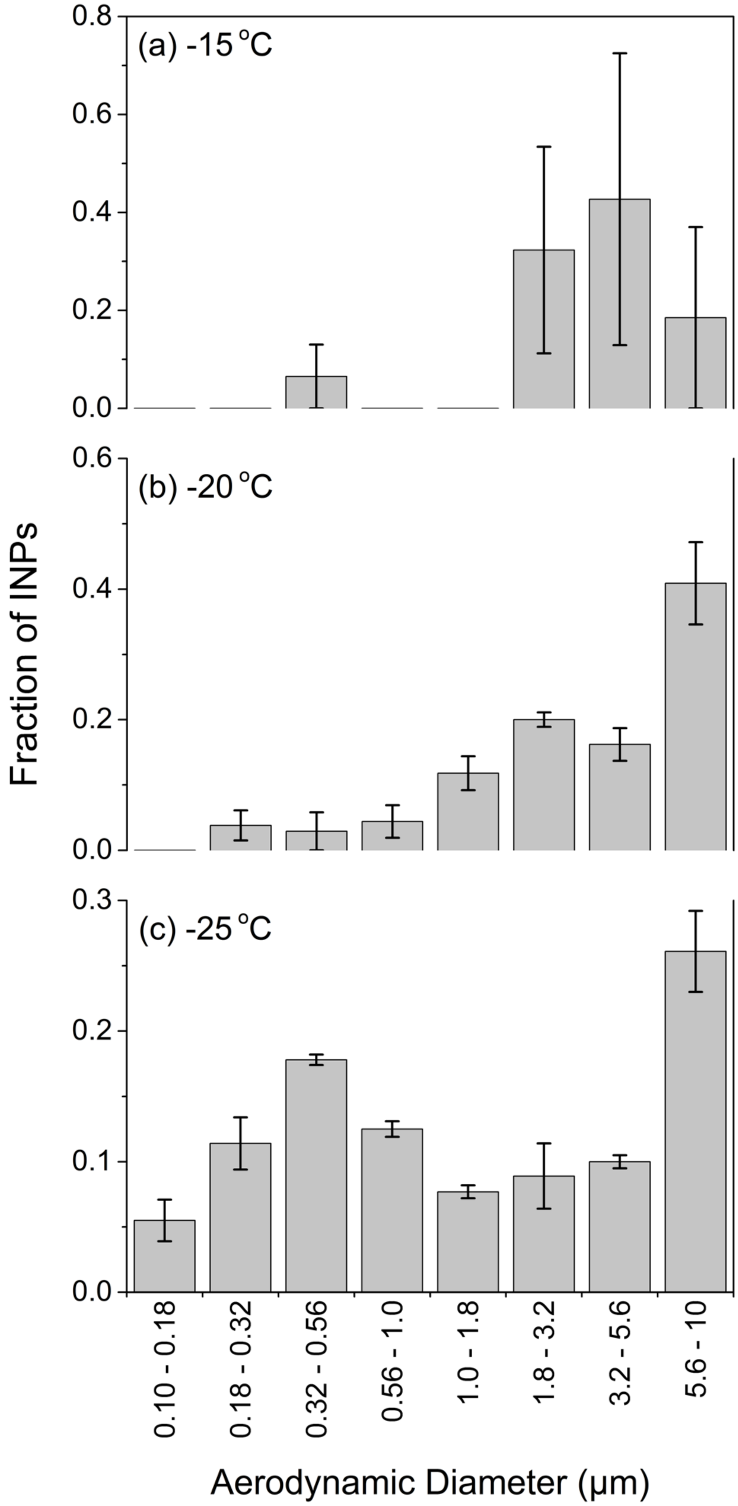

Figure S6. Mean INP size distributions at the UBC campus in BC, Canada at (a) -15 °C, (b) -20 °C, and (c) -25 °C. Here we report the fraction of INPs in each MOUDI size bin as the mean of all samples with uncertainty as the standard error of the mean.

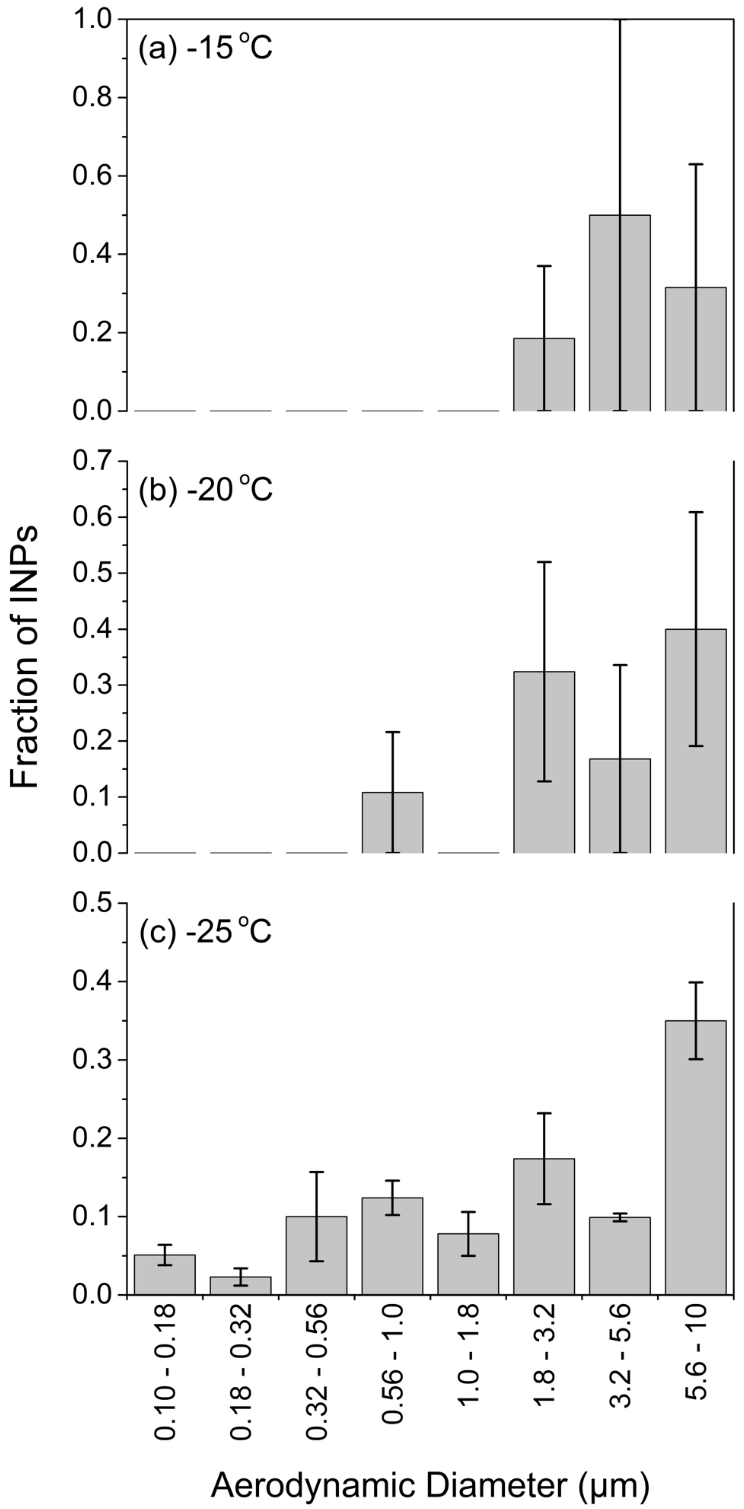

Figure S7. Mean INP size distributions at Colby, Kansas, USA at (a) -15 °C, (b) -20 °C, and (c) -25 °C. Here we report the fraction of INPs in each MOUDI size bin as the mean of all samples with uncertainty as the standard error of the mean.